iScience, Volume *24*

Supplemental information

BCL11B is positioned upstream of PLZF and RORγt to control thymic development of mucosal-associated invariant T cells and MAIT17 program

Theodore T. Drashansky, Eric Y. Helm, Nina Curkovic, Jaimee Cooper, Pingyan Cheng, Xianghong Chen, Namrata Gautam, Lingsong Meng, Alexander J. Kwiatkowski, William O. Collins, Benjamin G. Keselowsky, Derek Sant'Angelo, Zhiguang Huo, Weizhou Zhang, Liang Zhou, and Dorina Avram

Supplementary Information

Supplementary Figures

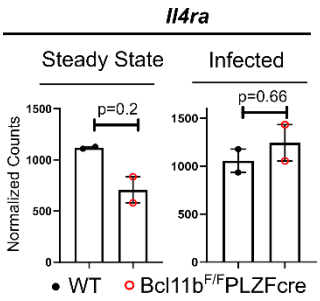

Figure S1, related to Figure 2. I*L4Ra* mRNA levels are high in MAIT cells and not altered by Bcl11b removal. DESeq2 normalized counts for *IL4Ra* in Bcl11b KO and WT MAIT cells in lung at steady state or following *Salmonella* infection. RNA-seq was performed on sorted lin- TCRβ +MR1t-5-OP-RU+ MAIT cells from lung of Bcl11b$^{F/F}$PLZFcre/R26R-EYFP mice and WT control mice at steady state or infected with *Salmonella* Typhimurium BRD509 (*Salmonella*) intranasally, day 7 post infection. For Bcl11b$^{F/F}$ PLZFcre/R26R-EYFP mice, in addition to lin- TCRβ + MR1t-5-OP-RU+, sorting was conducted on YFP+ cells. Additional details are provided in Fig. 5 and Material and Methods. False discovery rate (FDR)–adjusted *p* values were calculated using the Benjamini-Hochberg method with a significance cutoff of adjusted $p < 0.05$.

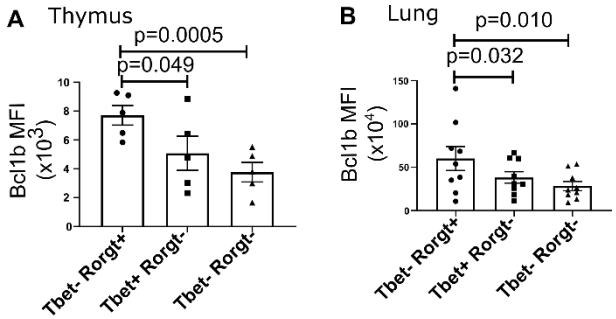

Figure S2, related to Figure 3. Bcl11b levels in MAIT functional subsets. (**A** and **B**) Bcl11b MFI in MAIT1, MAIT17 and double negative WT MAIT cells in the thymus (**A**) and lungs (**B**) of

uninfected mice. Student's t-test was used for statistical analysis. $p < 0.05$ was considered significant.

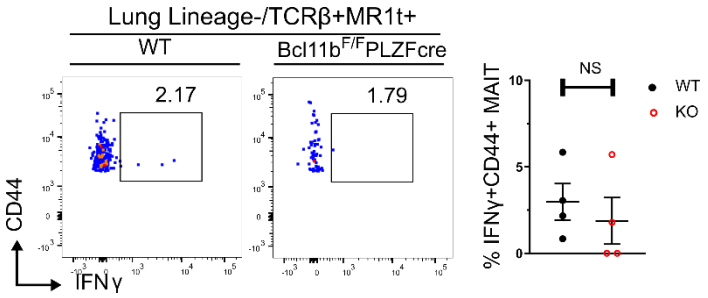

Figure S3, related to Figure 3. IFNγ levels are low and equal in Bcl11b KO and WT MAIT cells at steady state. Representative dot plots (left) and frequencies (right) of Bcl11b KO and WT IFNγ+CD44+ MR1t-5-OP-RU+ TCRβ lin- MAIT cells in lung at steady state. Each point represents a concatenated file of 2 lung samples run independently. Statistics were conducted as paired t-test. $p < 0.05$ was considered significant.

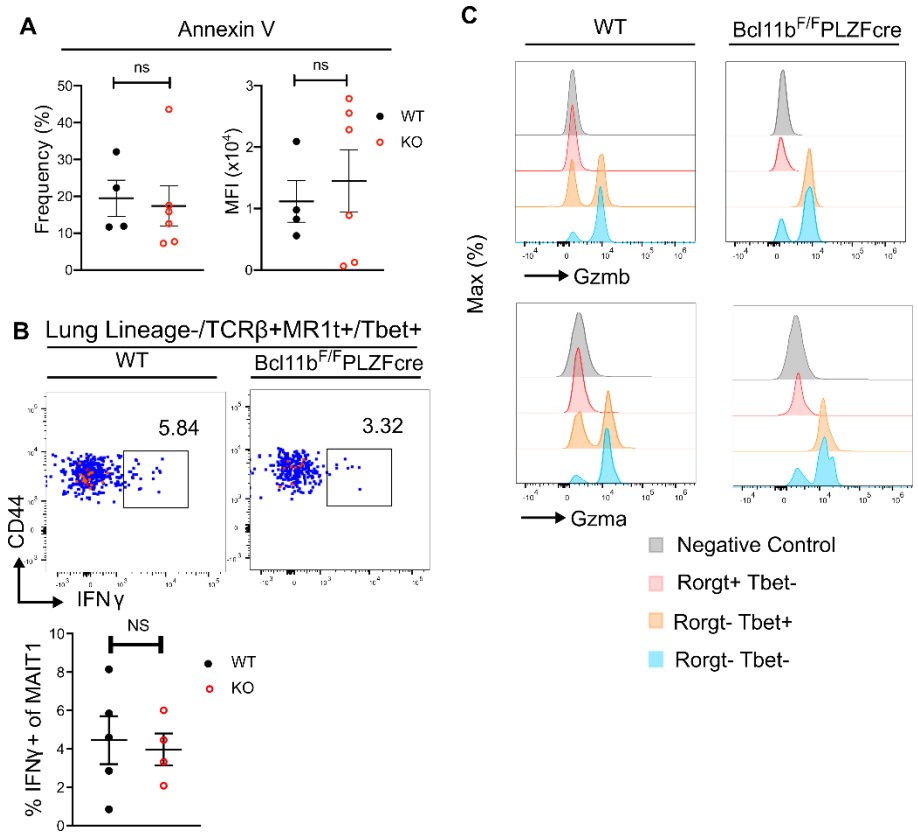

Figure S4, related to Figure 4. Analysis of Bcl11b KO and WT MAIT cells following *Salmonella* BRD509 infection. Bcl11b$^{F/F}$ PLZFcre and WT mice were infected with *Salmonella* BRD509 intranasally and euthanized 7 days post infection. (**A**) Frequencies and MFI of Annexin V staining of Bcl11b KO and WT MR1t-5-OP-RU+ MAIT cells in the lung following *Salmonella* infection. (**B**) Representative dot plots and frequencies of IFNγ+CD44+ MR1t-5-OP-RU+ MAIT cells following *Salmonella* infection. (**C**) Representative histograms of GzmB and GzmA staining in Bcl11b KO and WT MAIT17, MAIT1 and Rorγt-Tbet- MR1t-5-OP-RU+ MAIT cells in the lung of infected mice. Negative control represents gated lineage+ TCRβ- cells. Statistics were conducted as paired t-test. $p < 0.05$ was considered significant.

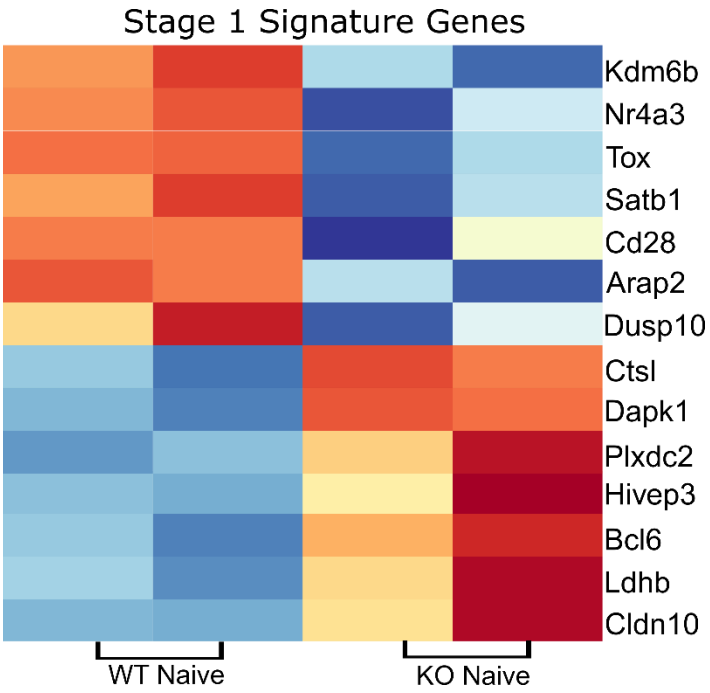

Figure S5, related to Figure 5. Stage 1 signature genes in lung MAIT cells in the absence of Bcl11b. RNA-seq was performed on sorted lin- TCRβ + MR1t-5-OP-RU+ MAIT cells from lung of Bcl11b$^{F/F}$PLZFcre/R26R-EYFP mice and WT control mice at steady state. For Bcl11b$^{F/F}$ PLZFcre/R26R-EYFP mice, in addition to TCRβ +MR1t+, sorting was conducted on YFP+ cells. Heatmaps of differentially expressed stage 1 genes in lung Bcl11b KO and WT MR1t-5-OP-RU+ MAIT cells at steady state.

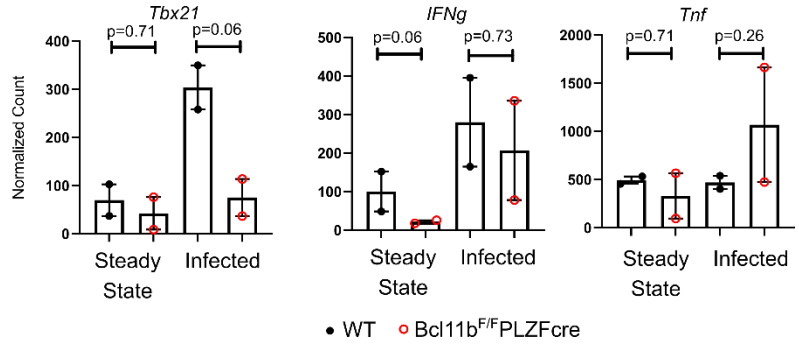

Figure S6, related to Figure 5. MAIT1 genes are not significantly altered in the absence of Bcl11b at steady state or following infection. DESeq2 normalized counts for *Tbx21, Ifn*γ and *Tnf* in Bcl11b KO and WT MAIT cells in lung at steady state or following *Salmonella* infection. RNA-seq was performed on sorted lin- TCRβ +MR1t-5-OP-RU+ MAIT cells from lung of Bcl11b$^{F/F}$PLZFcre/R26R-EYFP mice and WT control mice at steady state or infected with *Salmonella* Typhimurium BRD509 (*Salmonella*) intranasally, day 7 post infection. For Bcl11b$^{F/F}$ PLZFcre/R26R-EYFP mice, in addition to lin- TCRβ+ MR1t-5-OP-RU+, sorting was conducted on YFP+ cells. Additional details are provided in Fig. 5 and Material and Methods. False discovery rate (FDR)–adjusted *p* values were calculated using the Benjamini-Hochberg method, with a significance cutoff of adjusted $p < 0.05$.

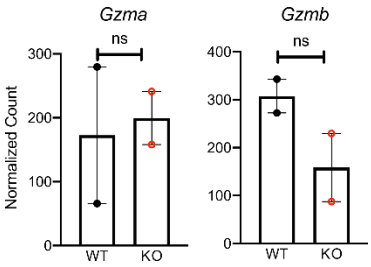

Figure S7, related to Figure 5. Granzyme mRNAs are unaffected by Bcl11b deletion in MAIT cells. DESeq2 normalized counts for *Gzma* and *Gzmb* in lung of Bcl11b KO and WT

MAIT cells from *Salmonella* infected mice. RNA-seq was performed on sorted lin- TCRβ +MR1t-5-OP-RU+ MAIT cells from lung of Bcl11b$^{F/F}$PLZFcre/R26R-EYFP mice and WT control mice at steady state or infected with *Salmonella* Typhimurium BRD509 (*Salmonella*) intranasally, day 7 post infection. For Bcl11b$^{F/F}$ PLZFcre/R26R-EYFP mice, in addition to lin- TCRβ + MR1t-5-OP-RU+, sorting was conducted on YFP+ cells. Additional details are provided in Fig. 5 and Material and Methods. False discovery rate (FDR)–adjusted *p* values were calculated using the Benjamini-Hochberg method, with a significance cutoff of adjusted $p < 0.05$.

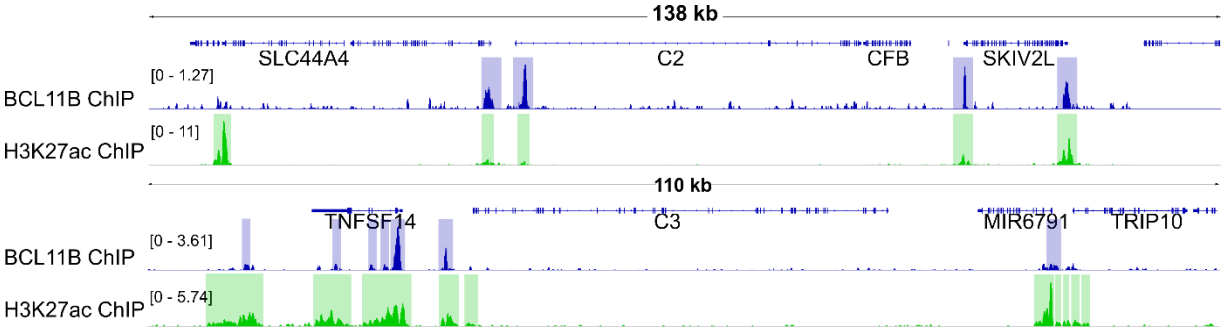

Figure S8, related to Figure 8. Bcl11b binding ant H3K27Ac at *C2* and *C3* complement loci in human MAIT cells from healthy donors. IGV visualization of *C2* and *C3* loci from Bcl11b ChIP-seq (track 1) and H3K27Ac (track 2) human MAIT cells. Blue and green highlights indicate significant ChIP-seq peaks. ChIP-seq scale bar normalized to sequences per million reads.

Table S3. MAIT17 program genes and differential expression at steady state or infection (compiled from Koay et al. 2019), **related to Figure 5**.

Genes	**DEG in Bcl11b KO versus WT - steady state**	**DEG in Bcl11b KO versus WT - infection**
Blk	down	down
Pxdc1	down	down
S100a4	down	down
Actn2	down	down
Aqp3	down	NC
Cd7	down	NC
Apol7b	down	down
Tnfrsf25	down	down
Stab2	down	NC
Emb	down	down
Sdc1	down	NC
Itgae	down	down
Ramp1	down	down
Ramp3	down	down
Icos	down	down
Il27ra	down	down
Il12rb	down	down
Cd44	down	down
Ccr2	down	down
Zbtb16	down	down
Maf	down	down
Il7r	down	down
Il18r1	down	down
Il17a	down	down
Il23r	down	down

Il17rb	down	down
Il1r1	down	down
Il17re	down	down
Rorc	down	down
Ccr6	down	down
Tmem176a	NC	NC
Serpinb1a	NC	down
Tmem176b	NC	NC
Lrrc17	NC	NC
Lrrc58	NC	NC
Cabin1	NC	down
Chad	NC	NC
Kcnk1	NC	NC
Avpi1	NC	NC
Prelid1	NC	NC
Jag1	NC	up
Mycn	NC	NC
Rnf208	NC	down
Il17f	NC	down
Il22	NC	NC
Cxcl2	NC	up
Iltifb	NC	NC

Table S4. MAIT1 program genes and differential expression at steady state or infection (compiled from Koay et al. 2019), **related to Figure 5**.

Genes	**DEG in Bcl11b KO versus WT - steady state**	**DEG in Bcl11b KO versus WT - infection**
Klrk1	NC	NC
Fgl2	down	NC
Cd28	down	down
Il2rb	down	down
Satb1	down	NC
Nkg7	NC	NC
Klrd1	NC	NC
Ly6c2	NC	up
Klrb1c	NC	NC
Gzmb	NC	NC
Gimap3	NC	NC
Klra3	NC	NC
Ms4a4b	NC	NC
Klra9	NC	NC
AW112010	NC	NC
Slamf7	NC	up
Klrc2	NC	NC
Hsd11b1	NC	NC
H2-Q6	NC	NC
Stat4	NC	down
Klra5	NC	NC
Klrc1	NC	NC
Styk1	NC	NC
Klra13-ps	NC	NC
Itga4	NC	NC

H2-K1	NC	NC
Klra6	NC	NC
Klra8	NC	NC
Klra10	NC	NC
Klrc2	NC	NC
Klre	NC	NC
Ugcg	NC	NC
Inpp4b	NC	NC
Bcl2	NC	NC
Itm2a	NC	NC
Ccl5	NC	NC
Ifng	NC	NC
Il21r	NC	NC
Xcl1	NC	NC
Cxcr3	NC	down
Ccl4	NC	up
Ccr9	NC	NC
Ccl3	NC	up
Lef1	NC	NC
Il10ra	NC	up
Il18rap	NC	NC
Cxcr4	NC	NC

Table S5. CD4+Lef1+CD138-CD319- early stage 3 precursor program genes and differential expression at steady state or infection (compiled from Koay et al. 2019), **related to Figure 5**.

Genes	DEG in Bcl11b KO versus WT - steady state	DEG in Bcl11b KO versus WT - infection
Satb1	down	NC
Tcf7	down	down
Cd4	NC	up
Lef1	NC	NC
Itm2a	NC	NC
Cd27	NC	NC

Table S6. TCR Signaling pathway genes and differential expression at steady state or infection, related to Figure 5.

Genes	DEG in Bcl11b KO versus WT - steady state	DEG in Bcl11b KO versus WT - infection
Pdpk1	NC	NC
Bcl10	NC	NC
Cd247	NC	NC
Cd28	down	down
Cd3d	down	Down
Cd3e	down	Down
Cd3g	down	Down
Cd4	NC	up
Cd40l	down	down
Cd8a	NC	NC
Cd8b1	NC	NC
Fos	NC	NC
Fyn	NC	down
Grap2	down	down
Hras	NC	NC
Itk	down	down
Kras	NC	NC
Malt1	NC	up
Rasgrp1	down	Down
4930544G11Rik	NC	NC
Card11	down	Down
Cdc42	NC	NC
Csf2	NC	NC
Chuk	NC	NC
Cdk4	NC	NC
Ctla4	NC	down
Dlg1	NC	NC
Gsk3b	NC	NC

Grb2	NC	NC
Icos	down	down
Ikbkb	NC	NC
Ikbkg	NC	NC
Ifng	NC	NC
Jun	NC	NC
Lat	down	down
Lck	down	down
Mapk1	NC	NC
Mapk11	NC	NC
Mapk12	NC	NC
Mapk13	up	NC
Mapk14	NC	NC
Mapk3	NC	NC
Map2k1	NC	NC
Map2k2	NC	NC
Map2k7	NC	NC
Map3k14	down	down
Map3k7	NC	NC
Map3k8	NC	NC
Nras	NC	NC
Nck1	NC	NC
Nck2	NC	NC
Nfatc1	down	Down
Nfatc2	NC	Down
Nfatc3	down	down
Nfkb1	NC	NC
Nfkbia	NC	NC
Nfkbib	NC	NC
Nfkbie	Down	NC
Pak1	NC	up
Pak2	NC	NC
Pak3	NC	NC
Pak4	NC	NC
Pak5	NC	NC
Pak6	NC	NC
Pak7	NC	NC
Pik3r3	NC	NC
Pik3cd	down	NC
Pik3ca	NC	NC
Pik3cb	NC	up
Pik3r1	NC	NC
Pik3r2	NC	Up
Pik3cg	down	NC
Pik3r5	NC	NC
Plcg1	NC	down
Pdcd1	down	down
Ppp3ca	NC	NC
Ppp3cb	NC	down

Ppp3cc	NC	NC
Ppp3r1	NC	NC
Ppp3r2	NC	NC
Ptpn6	NC	NC
Ptprc	down	NC
Rhoa	NC	NC
Sos1	NC	NC
Sos2	NC	NC
Tec	NC	NC
Raf1	NC	NC
Rela	NC	NC
Vav1	NC	NC
Vav2	NC	NC
Vav3	NC	up
Zap70	down	down

Table S7. Key Resources Table. Antibodies.

Antibody	SOURCE	IDENTIFIER
Anti-mouse T-bet, BV421	Biolegend	Cat #: 644816
Anti-mouse granzyme A, eFluor450	eBioscience	Cat #: 48-4831-82
Anti-mouse CD45.2 eFluor506	eBioscience	Cat #: 69-0454-82
Anti-mouse CD44, BV510	Biolegend	Cat #: 103044
Anti-mouse TCRβ, Super Bright 600	eBioscience	Cat #: 63-5961-82
Anti-mouse B220, BV650	Biolegend	Cat #: 103241
Anti-mouse CD11c, BV650	Biolegend	Cat #: 117339
Anti-mouse GR1, BV650	Biolegend	Cat #: 108442
Anit-mouse CD45.1, Super Bright 702	eBioscience	Cat #: 67-0453-82
Anti-mouse TNF, BV750	Biolegend	Cat #: 506358
Anti-mouse IFNγ, BV785	Biolegend	Cat #: 17-6988-82
Anti-mouse MR1-5-OP-RU, PE or APC	NTCF	N/A
Anti-mouse MR1-6-FP, PE or APC	NTCF	N/A
Anti-mouse granzyme B, PE/CF594	BD Biosciences	Cat #: 562462
Anti-mouse IL-17A, PE/cy7	eBioscience	Cat #: 25-7177-82
Anti-mouse/human Bcl11b, rabbit	Bethyl Labs	Cat #: A300-385A
Goat-anti-rabbit secondary, AlexaFluor488	ThermoFisher	Cat #: A11008
Anti-mouse PLZF, PerCP/cy5.5	Biolegend	Cat #: 145808
Anti-mouse Rorγt, APC	eBioscience	Cat #: 17-6988-82

Fixable viability dye, eFluor780	eBioscience	Cat #: 65-0865-14
Anti-mouse CD8a, Super Bright 702	eBioscience	Cat #: 67-0081-82
Anti-mouse Ki67, AlexFluor700	Biolegend	Cat #: 652420
Annexin V, Pacific Blue	eBioscience	Cat #: 640918
Anti-human CD3, PerCP/cy5.5	Biolegend	Cat #: 317338
Anti-human CD161, PE/Texas Red	Biolegend	Cat #: 339940
Anti-human TCRVα7.2, BV421	Biolegend	Cat #: 351716
Anti-human CD4, Biotin	Biolegend	Cat #: 317438
Anti-human CD11b, Biotin	Biolegend	Cat #: 301304
Anti-human CD14, Biotin	Biolegend	Cat #: 301826
Anti-mouse T-bet, PE/cy7	eBioscience	Cat #: 25-5825-82
Anti-mouse CD24, BV605	Biolegend	Cat #: 101827
Anti-mouse CD69, PerCP/cy5.5	Biolegend	Cat #: 104522
Anti-mouse CD8a, BV785	Biolegend	Cat #: 100750
Anti-mouse CD44, APC/cy7	Biolegend	Cat #: 103028
Anti-mouse TCRβ, eFluor450	eBioscience	Cat #: 48-5961-82
Anti-mouse CD62L, BV711	Biolegend	Cat #: 104445
Anti-Streptavidin, PE	Agilent	Cat #: PJRS25

Transparent Methods

Mice. PLZFcre^{+} mice (Zhang et al. 2015) were bred with Bcl11b$^{F/F}$ mice, on a C57BL/6 background, to generate Bcl11b$^{F/F}$ PLZFcre+ (KO) and Bcl11b$^{F/F}$ (WT) mice and further with R26R-EYFP mice to generate Bcl11b$^{F/F}$ PLZFcre/R26R-EYFP mice. Both males and females of 6-8 weeks of age were used in all experiments conducted. Littermates of the same sex were used, as WT and KO mice. Mice were bred and maintained under specific pathogen-free conditions and kept in-house for experiments in individually ventilated cages under specific pathogen-free conditions. All experiments were conducted according to animal protocols approved by Institutional Animal Care and Use Committees of University of Florida, Moffitt Cancer Center and University of South Florida.

Salmonella Typhimurium BRD509 Infections. *Salmonella enterica* ser. Typhimurium BRD509 was provided by Dr. Stephen J. McSorley of UC- Davis. 10^6 cfu of *Salmonella* was instilled intra-nasally and mice were euthanized after 7 days.

Human Subjects. PBMCs derived buffy coats of healthy volunteers were purchased from LifeSouth Community Blood Centers. MAIT cells were sorted as CD3+CD161+TCRVα7.2+ cells.

Bone Marrow Chimeras. Cells were isolated from bone marrows (BM) of $Bcl11b^{F/F}$ PLZF-Cre^{+} (KO) (CD45.2) and WT (CD45.1/2) mice and mixed at a 1:1 ratio. 10 million BM cells were injected i.v. into lethally irradiated CD45.1 recipient mice. Prior to transfer CD45.1 mice were irradiated 2 times, 4 hours apart with 550 rad. Mice were analyzed 8 weeks post-transplant.

MR1 tetramer. Biotinylated MR1-5-OP-RU and MR1-6-FP monomers were obtained from the National Institutes of Health Tetramer Core Facility and were tetramerized with Strepavidin-PE or -APC. Tetramer was titrated on WT MAIT cells form thymus and lung.

Cell Isolation and analysis. Cell isolation was performed as previously described by VanValkenburgh *et al.*(Vanvalkenburgh et al. 2011). Briefly, cells from all lymphoid organs were placed on 40 µm filter and pressed through the filter while washed with 1% FBS complete RPMI medium. Lungs were processed using the gentleMACS Dissociator in 1% FBS complete RPMI medium with 10mg/mL of Collagenase A and 5µg/mL of DNAse I with the protocol for setting Lung 1, followed by for 30 minutes incubation at 37C with shaking at 220rpm. Digestion was stopped with 50 µL of 0.5M of EDTA. and further Lung setting 2 protocol was conducted. Tissue was passed through 40 µm filter and washed with additional 1% FBS complete RPMI medium, centrifuged at 350 *x g* for 10 minutes. The pellets were resuspended in 30% Percoll and layered on top of 70% Percoll and centrifuged at 2500rpm for 20 minutes. For analysis of cytokine production, cells were resuspended in 10% complete RPMI media at a concentration of 1 x 10^8

cells/ml in the presence of PMA and ionomycin, at a final concentration of 25ng/ml and 1µg/mL, respectively for 5 hours with Brefeldin A added to a final concentration of 0.3µM, for the last 4 hours.

For thymic MAIT cells only, a CD8+ T cell negative selection enrichment kit was used in total thymocytes, given that in the thymus MAIT cells are rarely CD4+ or DP.

For the lung cells, no enrichment was used, however cells were stained with a cocktail of B220, Gr1, Cd11b (all PE-Cy7) (dump gate, (lin+)), as well as for TCRβ and with MR1t-5-OP-RU. TCRβ and with MR1t-5-OP-RU+ cells were analyzed in the lin- population.

Antibodies and fluorophores information is provided in Table S7.

RNA-seq library preparation. RNA was extracted from sort-purified WT and Bcl11b KO (YFP+) lin- TCRβ + MR1t-5-OP-RU+ MAIT cells from *Salmonella* BRD509 infected or unifected $Bcl11b^{F/F}$ (WT) and $Bcl11b^{F/F}$ $PLZFcre^{+}$ $Rosa26YFP^{+}$ mice, using the RNeasy Plus Micro Kit (QIAGEN 74034), and rRNA was depleted using NEBNext rRNA Depletion Kit (NEB E63102). cDNA libraries were prepared using NEBNext Ultra II RNA Library Prep Kit (NEB E7770S), quality was assessed on a Bioanalyzer (Agilent, #5067-4626), and sequenced on a HiSeq3000 at approximately 30 million reads per library.

BCL11B ChIP-seq. Human MAIT cells were sort purified from PBMCs as CD3+CD161+TCRVα7.2+ cells derived from nine donors. ChIP-Seq against Bcl11b was performed on MAIT cells using the SimpleChIP Enzymatic Chromatin IP Kit from Cell Signaling Technologies (CST #9003), following their recommended protocol up to the library preparation with the following alterations: (1) 10^7 cells were used in place of 4×10^7; (2) formaldehyde fixation was performed in 1 mL; (3) Buffer A and Buffer B steps were performed in 1 mL; (4) cells were sheared in ChIP-buffer to an average of 200-1000bp using a Diagenode Bioruptor Pico (Diagenode B01060002); (5) a cocktail of 3 anti-Bcl11b antibodies

were used (8mg ab18465, 8 mg of CST #12120 and 8mg of Bethyl A300-385 per ChIP); (6) final DNA purification was performed by phenol:chloroform:isoamyl alcohol extraction with MaXtract high density columns (Qiagen #129046). Libraries were prepared using NEBNext Ultra II DNA Library Prep Kit (NEB #E7645S) and sequenced as PE 2x100 on a HiSeq3000.

H3K27ac ChIP-seq. ChIP-seq for H3K27ac was performed on two independent samples derived from two donors. 100,000 sort purified human MAIT cells (CD3+CD161+TCRVα7.2+ using the Low Cell ChIP-Seq kit from Active Motif (#104895) following strictly the manufacturer's recommended protocol scaled to 100,000 cells. H3K27ac antibody was from Cell Signaling Technologies (#8173) at the recommended 1:100 dilution. Libraries were run as PE 2x100 on a HiSeq3000.

QUANTIFICATION AND STATISTICAL ANALYSIS

RNA-seq Data Processing. RNA-seq fastq files were trimmed using seqtk and the quality assessed using FastQC (Lorentsen et al. 2018). The trimmed reads were aligned to the mouse genome (mm10) using Hisat2 and transcript counts were obtained using HTseq (Lorentsen et al. 2018). DeSeq2 was used for differential expression analysis (Lorentsen et al. 2018). Significance for RNA-seq data was determined using DeSeq2 (Love, Huber and Anders 2014).

ChIP-seq data Processing. Data analysis for ChIP-seq was performed using a customized pipeline based on a previously published version (Lorentsen et al. 2018). Briefly, fastq files were first trimmed using Trimmomatic and read quality was assessed using FastQC. Reads were aligned to the mouse genome (mm10) using Bowtie2. The resulting SAM file was pruned (Q>30), converted to BAM format and was sorted using SAMtools. Duplicate reads were removed using Picard tools and MACS2 was used for peak calling and bedgraph file preparation. Bedgraph files were visualized using Integrative Genomics Viewer (IGV).

Statistics. For the Spearman Correlation plot, tag counts of each peak in Bcl11b and H3K27ac and peak annotation were obtained using HOMER software. Correlation in the tag counts

between Bcl11b and H3K27ac was evaluated using the Spearman's method. P-value was obtained from Student's t-test to examine if the correlation was significant and analysis was carried out in R. For all mouse experiments where the mice were not infected with *Salmonella* BRD509, two files were concatenated to create individual points on the frequency statistics graphs and for representative figures. For all flow cytometry experiments data was analyzed in GraphPad Prism. For single comparisons, we used two-tailed Student's *t*-test, and $p<0.05$ were considered significant. In case of multiple groups of mice of different phenotypes, we used an analysis of variance or a Kruskal-Wallis test applicable for continuous variables.

References

Koay, H. F., S. Su, D. Amann-Zalcenstein, S. R. Daley, I. Comerford, L. Miosge, C. E. Whyte, I. E. Konstantinov, Y. d'Udekem, T. Baldwin, P. F. Hickey, S. P. Berzins, J. Y. W. Mak, Y. Sontani, C. M. Roots, T. Sidwell, A. Kallies, Z. Chen, S. Nussing, K. Kedzierska, L. K. Mackay, S. R. McColl, E. K. Deenick, D. P. Fairlie, J. McCluskey, C. C. Goodnow, M. E. Ritchie, G. T. Belz, S. H. Naik, D. G. Pellicci & D. I. Godfrey (2019) A divergent transcriptional landscape underpins the development and functional branching of MAIT cells. *Sci Immunol,* 4 (41):eaay6039

Vanvalkenburgh, J., D. I. Albu, C. Bapanpally, S. Casanova, D. Califano, D. M. Jones, L. Ignatowicz, S. Kawamoto, S. Fagarasan, N. A. Jenkins, N. G. Copeland, P. Liu & D. Avram (2011) Critical role of Bcl11b in suppressor function of T regulatory cells and prevention of inflammatory bowel disease. *J Exp Med,* 208**,** 2069-81.

Koay, H. F., S. Su, D. Amann-Zalcenstein, S. R. Daley, I. Comerford, L. Miosge, C. E. Whyte, I. E. Konstantinov, Y. d'Udekem, T. Baldwin, P. F. Hickey, S. P. Berzins, J. Y. W. Mak, Y. Sontani, C. M. Roots, T. Sidwell, A. Kallies, Z. Chen, S. Nussing, K. Kedzierska, L. K. Mackay, S. R. McColl, E. K. Deenick, D. P. Fairlie, J. McCluskey, C. C. Goodnow, M. E. Ritchie, G. T. Belz, S. H. Naik, D. G. Pellicci & D. I. Godfrey (2019) A divergent transcriptional landscape underpins the development and functional branching of MAIT cells. *Sci Immunol,* 4.

Lorentsen, K. J., J. J. Cho, X. Luo, A. N. Zuniga, J. F. Urban, Jr., L. Zhou, R. Gharaibeh, C. Jobin, M. P. Kladde & D. Avram (2018) Bcl11b is essential for licensing Th2 differentiation during helminth infection and allergic asthma. *Nat Commun,* 9**,** 1679.

Love, M. I., W. Huber & S. Anders (2014) Moderated estimation of fold change and dispersion for RNA-seq data with DESeq2. *Genome Biology,* 15**,** 550.

Vanvalkenburgh, J., D. I. Albu, C. Bapanpally, S. Casanova, D. Califano, D. M. Jones, L. Ignatowicz, S. Kawamoto, S. Fagarasan, N. A. Jenkins, N. G. Copeland, P. Liu & D. Avram (2011) Critical role of Bcl11b in suppressor function of T regulatory cells and prevention of inflammatory bowel disease. *J Exp Med,* 208**,** 2069-81.

Zhang, S., A. Laouar, L. K. Denzin & D. B. Sant'Angelo (2015) Zbtb16 (PLZF) is stably suppressed and not inducible in non-innate T cells via T cell receptor-mediated signaling. *Sci Rep,* 5**,** 12113.